

## Supporting Information

### Synthesis of samples

Sn pellets (99.5%), S crystals (99.9996%), and  $\alpha$ -Dy<sub>2</sub>S<sub>3</sub> powder (99%) were used to grow the whiskers. The synthesis of SnS and experimental details of SnS evaporation can be found in <sup>19</sup>. A mixture of SnS (95 mol.%) and 0.3 g  $\alpha$ -Dy<sub>2</sub>S<sub>3</sub> (5 mol. %) was placed in a graphite crucible. The crucible was placed in a quartz ampoule, which was evacuated to 1 Pa and then sealed. The ampoule was placed in a horizontal dual-zone resistance furnace and heated to 1100 °C at a rate of approximately 2000 °C·h<sup>-1</sup>, held at this temperature for 12 h for the dissolution of Dy<sub>2</sub>S<sub>3</sub> into SnS melt. Then, the temperature of the reactor, which was used to condense SnS vapor, was decreased to 1070 °C. Due to the temperature difference, SnS flux from the hot region to the cold region occurred. Consequently, Dy<sub>2</sub>S<sub>3</sub> concentration in the graphite crucible increased, leading to its crystallization from the solution. This regime was held for 3 days. Then, the temperature in the cold part was decreased to 900 °C. This procedure enabled the complete removal of the residual SnS flux from the grown crystals in 3 h. The reactor was then pulled out from the furnace and quenched in iced water. The described preparation method results in a dark red sample comprising bulk  $\gamma$ -Dy<sub>2</sub>S<sub>3</sub> as well as its single-crystal whiskers. The morphology and size of whisker crystals growing on the surface of bulk  $\gamma$ -Dy<sub>2</sub>S<sub>3</sub> are shown in Figure 1 (**PGME**).

Additional experiments were carried out to determine the growth mechanism of  $\gamma$ -Dy<sub>2</sub>S<sub>3</sub> whiskers. During these experiments, **CGME**, **CGVE**, **PG**, **PGV**, and **PGVE** were prepared.

*Preparation of **CGME** and **CGVE**.* The bulk crystals of  $\gamma$ -Dy<sub>2</sub>S<sub>3</sub> (~50 mg each) with graphite particles (3–100  $\mu$ m) on their surface were placed into two graphite crucibles. Both crucibles were placed in separate quartz ampoules. In one of the crucibles, 100 mg SnS was added to provide direct contact between bulk  $\gamma$ -Dy<sub>2</sub>S<sub>3</sub> and SnS melt during synthesis (**CGME**); for the other, an equal amount of SnS was placed at the bottom of the quartz ampoule, so no direct contact between bulk  $\gamma$ -Dy<sub>2</sub>S<sub>3</sub> and SnS melt occurred (**CGVE**). Ampoules were evacuated, sealed, and placed in the dual-zone furnace. The furnace was heated to and held at 1100 °C for 3 h. Then, a gradient of 50 °C on the length of the ampoules was created, and the crucibles with crystals were kept in the hot zone. After 48 h, the furnace was turned off. The images of the samples are shown in Figure S1.

*Preparation of PG, PGV, and PGVE.* **PG** consisted of  $\alpha$ -Dy<sub>2</sub>S<sub>3</sub> powder with evenly distributed graphite particles. For **PG** preparation, 200 mg  $\alpha$ -Dy<sub>2</sub>S<sub>3</sub> powder, 100 mg graphite, and 20 ml isopropanol were placed in a glass vial. Then, the vial was closed and sonicated using a sapphire ultrasonic bath (ultrasonic power: 150 W, frequency: 35 kHz) for 8 h. To prevent the thermal restacking of colloidal particles, samples were thermostated at 20–22 °C during ultrasonication. The resulting mixture was centrifuged for 30 min at 4500 rpm. The resulting precipitate was used in further experiments (**PG**, Figure 2a). This sample was annealed to obtain SnS vapor at 1100 °C for 72 h (**PGV**, Figure 2b). Consequently, SnS was evaporated from **PGV** due to annealing at 1100 °C for 5 h (**PGVE**). The upper and lateral surfaces of **PGVE** are shown in Figures 2c and 2d, respectively.

### Research methods

Micrographs were obtained by Field Emission Scanning Electron Microscopy (FESEM, JEOL JSM-6700 F). Analysis of the elemental composition (% mas.) was carried out using electron probe microanalysis (EPMA, JEOL JXA-8100, Japan) with an acceleration voltage of 20 kV and current of 30 nA. DyPO<sub>4</sub> was used as a standard for dysprosium, SnO<sub>2</sub> for tin, a stoichiometric single-crystal  $\gamma$ -Dy<sub>2</sub>S<sub>3</sub> for dysprosium and sulfur. Additionally, the whisker and bulk crystals were analyzed using energy dispersion X-ray analysis (EDXA, spectrometer TM-3000, Bruker). Dysprosium determination in the SnS condensate was performed by microwave plasma atomic emission spectrometry (MP-AES, spectrometer Agilent 4100 MP-AES, Agilent Technologies). The limit of detection for dysprosium in solid SnS was  $1 \cdot 10^{-2}$  % mas.

Single-crystal X-ray diffraction data were collected using Bruker X8 diffractometer (Mo K $\alpha$ -radiation, graphite monochromator, 0.5-mm collimator, Apex II CCD detector with a resolution of 512  $\times$  512 pixels, pixel size: 120  $\mu$ m). The measurement method included one standard 360°  $\phi$ -scan with a step of 0.5° (720 frames). This method is not necessary for structures with cubic symmetry, but it provides high-precision results in cell parameter calculations using instrumental parameters (detector orientation, detector center, and sample position). The temperature of the samples was held at 25 °C using Oxford Cryosystems Cryostream 800 Plus cryostat. The processing of the obtained single-crystal data (collection of diffraction reflexes, cell parameter calculation, and model refinement) was carried out using APEX3 v.2018-7.2 <sup>24</sup>.

## Results

### Crystal structure

Helical single-crystal data analyses resulted in 3665 individual diffraction reflections with  $I/I_{\sigma} > 10$ . 2971 of these reflections correspond to the body-centered cubic cell with  $a = 8.3265(6)$  Å (structural type:  $\text{Th}_3\text{P}_4$ ).

The single-crystal X-ray diffraction of the bulk crystal (oval grain with dimensions  $150 \mu\text{m} \times 130 \mu\text{m} \times 120 \mu\text{m}$ ) was performed using the same measurement method. The observed diffraction pattern of the helical crystal is similar to that obtained from the bulk sample. The refinement conducted using 2851 reflections with  $I/I_{\sigma} > 10$  resulted in  $a = 8.3174(4)$  Å, which is  $0.0091$  Å less than that of the helical crystal. The closeness of unit cell parameters of helical and bulk crystals indicates that both had the same composition. It is known that<sup>23</sup>,  $\text{Th}_3\text{P}_4$  structure for rare earth chalcogenides with  $\text{Ln}_2\text{X}_3$  composition has vacancies. Thus, structural and composition data suggest that the crystallochemical formula of the crystals is  $\text{Dy}_{2.5}\text{Sn}_{0.2}\square_{0.3}\text{S}_4$ , where  $\square$  are the vacancies in the cation sublattice when distributed statistically.

To determine the growth direction (Figure S3), additional 20 helical crystals of various shapes and sizes (grown in the same experiment) were studied (Figure S4). We found that 18 samples were single crystals, while the remaining 2 had split diffraction spots, indicating that each of them consisted of two slightly misaligned single-crystal domains. Nevertheless, all 20 crystals gave diffraction spots with interplanar distances of  $0.6$  Å or smaller, indicating their high degree of crystallinity. Out of 20 crystals, 9 had grown along the  $[100]$  direction, 6 along  $[111]$ , and 1 along  $[110]$ , while 4 did not have any specific growth direction. These results showed that the growth direction of helical crystals is not determined by crystal shape or size.  $[100]$  and  $[111]$  seem to be the preferred growth directions although other growth directions may also occur. Besides, a high degree of crystallinity is typical for all helical crystals.

### Chemical composition

A composition of bulk crystals has been determined using two different samples obtained in separate growth experiments. Quantitative data were collected from each

crystal from an area of  $\sim 1 \text{ mm}^2$ . The averaged (20 points were measured for each sample) results of composition analyses determined by EMPA are shown in Table 1. The reproducibility of the results obtained by EMPA and EDXA ensured excellent reliability of the analytical data for helical whiskers.

Table 1. Composition of crystals

Sample	Dy, % mas.	Sn, % mas.	S, % mas.	Total amount, % mas.
Bulk crystals (EMPA)	$73.1 \pm 0.6$	$4.1 \pm 0.6$	$22.6 \pm 0.1$	99.8
Bulk crystals (EDXA)	73.2	4.0	22.8	100 *
Helical crystals (EDXA)	73.2	4.3	22.5	100 *

\* The content of the determined elements was normalized to 100%.

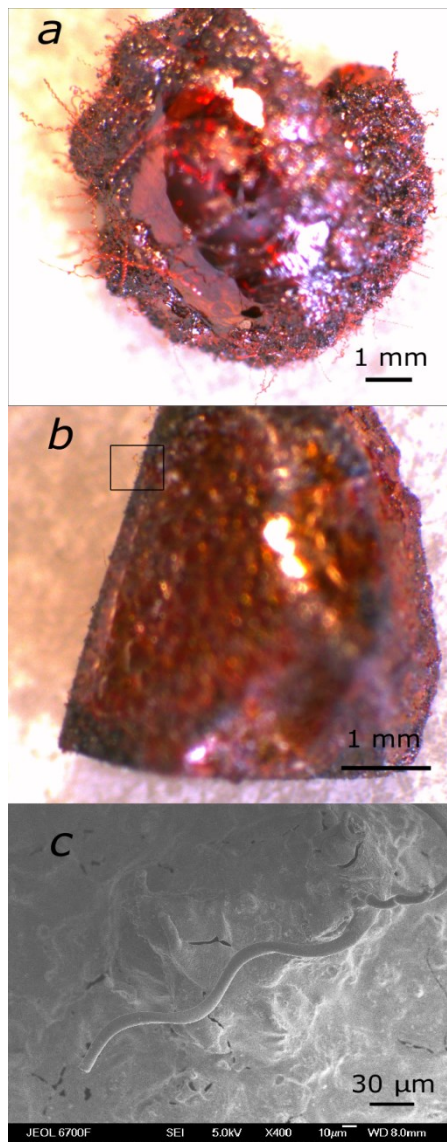


**Figure S1.** Photos of Samples: **CGME** (a) and **CGVE** (b). FESEM image of the **CGVE** surface (c).

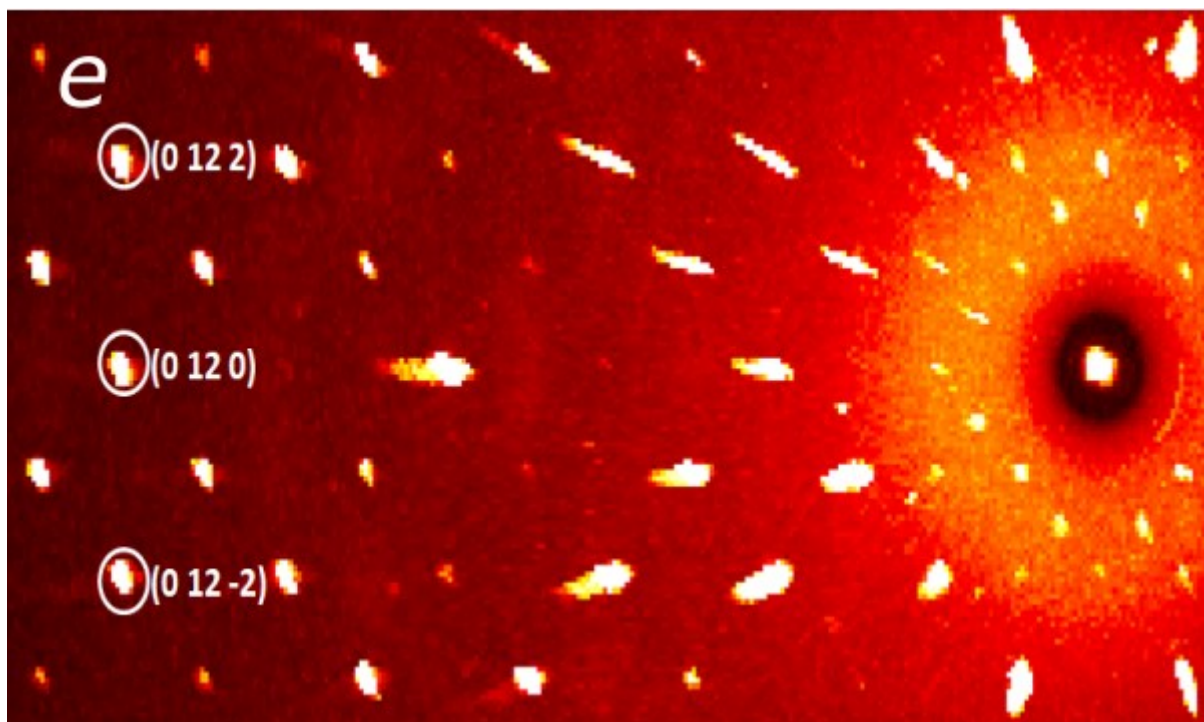


**Figure S2.** The selected area from Figure 3b with the Miller indices indicated.

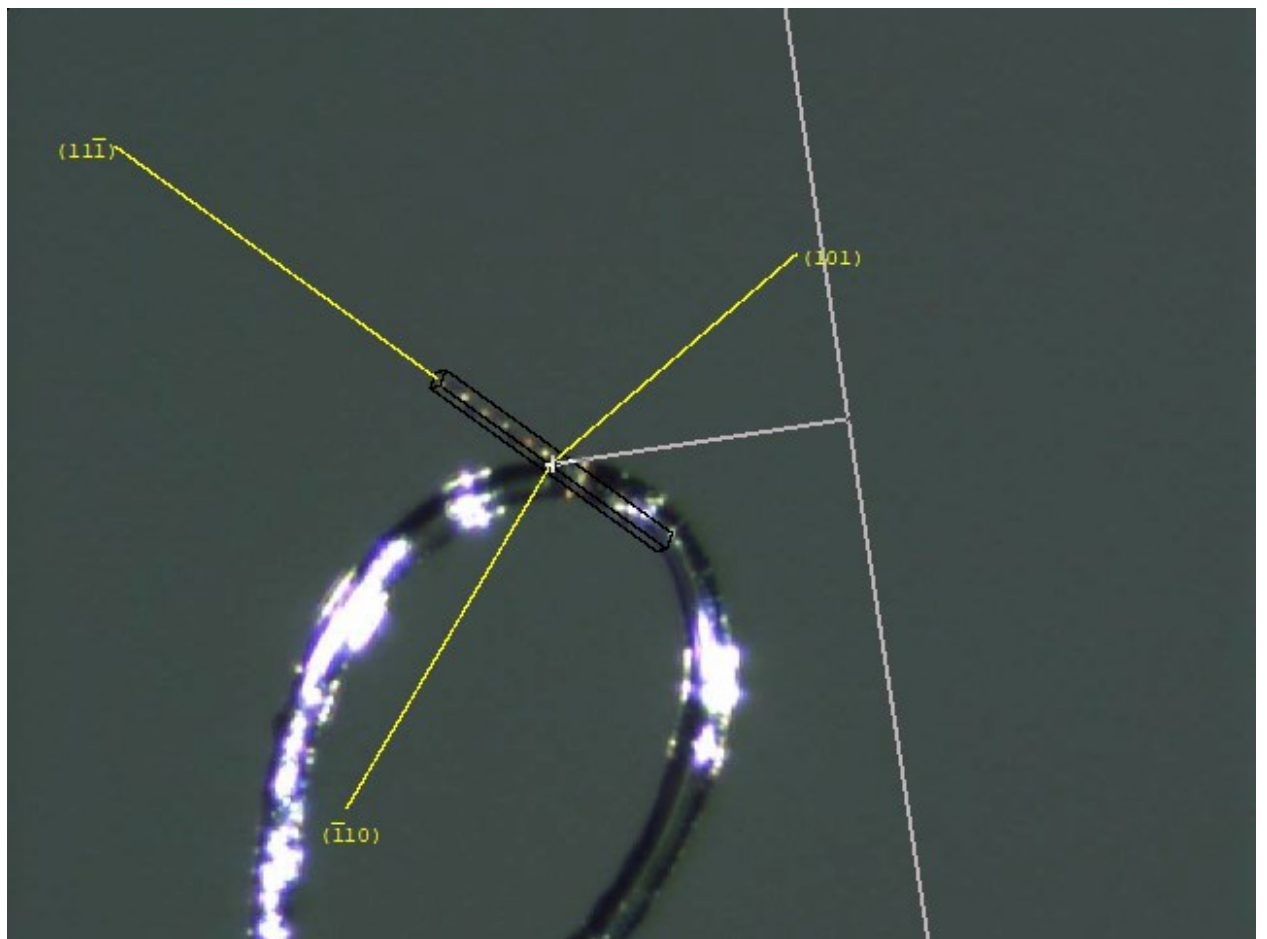


**Figure S3.** Helical  $\gamma$ - $\text{Dy}_2\text{S}_3$  single crystal with a growth direction of  $[111]$ .

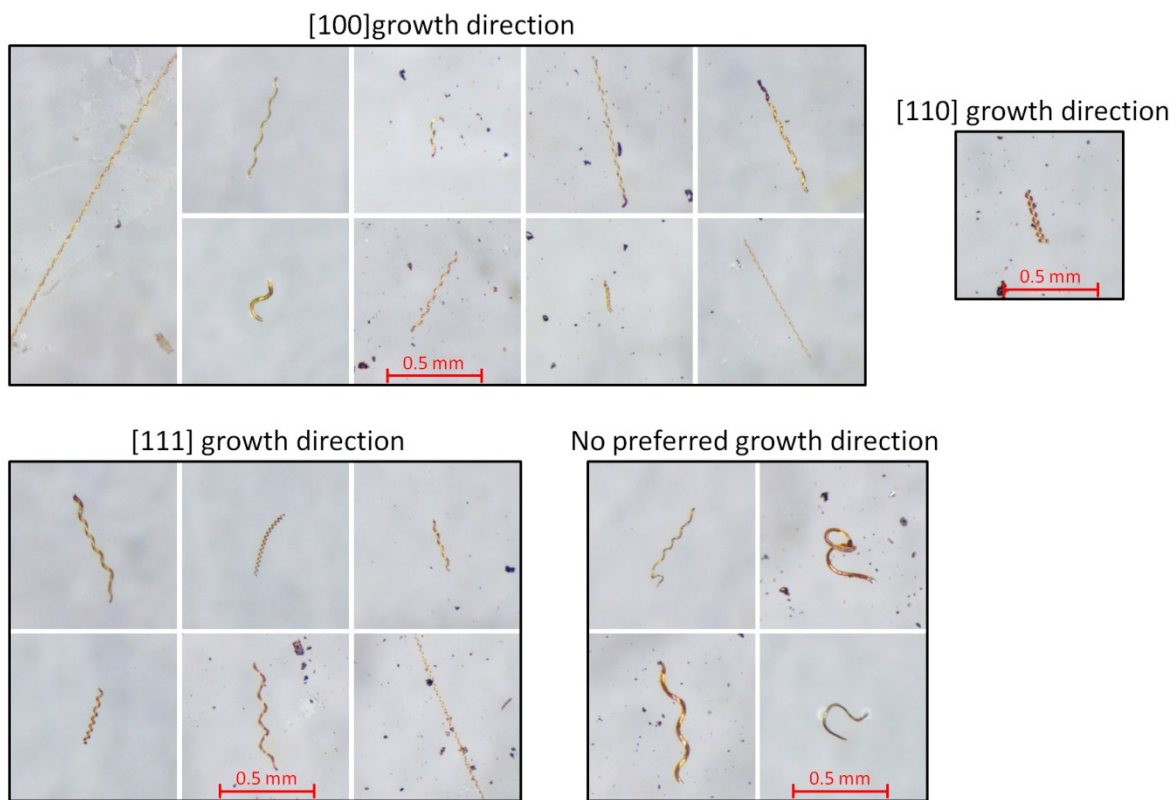


**Figure S4.** Growth directions of helical  $\gamma\text{-Dy}_2\text{S}_3$  single crystals.